



Cite this: *RSC Adv.*, 2020, **10**, 41618

2'-O-Methyl molecular beacon: a promising molecular tool that permits elimination of sticky-end pairing and improvement of detection sensitivity

Jiafeng Gao,^{†a} Yang Li,^{†b} Wenqin Li,^b Chaofei Zeng,^a Fengna Xi,^a Jiahao Huang^a and Liang Cui^a

An innovative 2'-O-methyl molecular beacon (MB) has been designed and prepared with improved thermal stability and unique nuclease resistance. The employment of 2'-O-methyl MBs helps efficiently suppress the background signal, while DNase I is responsible for the signal amplification and elimination of sticky-end pairing. The coupled use of 2'-O-methyl MBs and DNase I makes it possible to develop an enzyme-aided strategy for amplified detection of DNA targets in a sensitive and specific fashion. The analysis requires only mix-and-measure steps that can be accomplished within half an hour. The detection sensitivity is theoretically determined as 27.4 pM, which is nearly 200-fold better than that of the classic MB-based assay. This proposed sensing system also shows desired selectivity. All these features are of great importance for the design and application of MBs in biological, chemical, and biomedical fields.

Received 27th August 2020
 Accepted 20th October 2020

DOI: 10.1039/d0ra07341e
rsc.li/rsc-advances

Introduction

Developments in medical diagnosis require novel methods that are relatively simple and rapid, yet sufficiently sensitive and specific for DNA detection. Many DNA probes, including binary probes,¹ displacement probes,² TaqMan probes,³ and molecular beacons (MBs),⁴ have been applied for reliable determination of DNA targets. Among them, MBs have emerged as one of the most powerful and versatile molecular probes for biosensor constructions. An MB is a special hairpin DNA probe, which consists of a loop region for target recognition as well as a self-complementary stem domain with a fluorescence donor and acceptor tagged at the respective ends, which allow fluorescence resonance energy transfer (FRET) and thus realize signal production after forming a duplex with complementary DNA targets. Great progress has been made to apply MBs in biomedical detection due to the appealing features, such as high signal-to-background ratio, good molecular recognition specificity, and operation convenience without separation.^{5,6} However, MB-based assays still suffer from some inevitable limitations in some aspects. For example, the target-to-MB hybridization ratio and the DNA sticky-end pairing phenomenon are two typical disadvantages encountered by conventional MB-based methods, as shown in

Fig. 1. The intrinsic problem of target-to-MB binding in a 1 : 1 ratio (Fig. 1A) may greatly impede the signal acquisition and usually cause poor sensitivity of MB-based approaches. To overcome this limitation, it is highly demanded to incorporate signal amplification principles into the traditional MB-based sensing platforms.

To efficiently enhance detection sensitivities, there are some attractive options: nanomaterials-mediated strategies and enzyme-assisted methods. The detection qualities of MB-based methods have been notably benefited from the employment of promising nanomaterials, including gold nanoparticles,^{7,8} molybdenum disulfide nanosheets,^{9,10} silicon nanowires,¹¹ carbon nanotubes,¹² carbon nitride nanosheets,¹³ silver nanoparticles,¹⁴ and graphene.¹⁵ These nanomaterials can either serve as excellent fluorescence quenchers or be used as fantastic carriers for signaling probes. They facilitate the background suppression or signal amplification in conventional fluorescence MB-based methods, thereby leading to an enhanced sensitivity. However, problems still exist. For example, the preparation of nanomaterials are usually rather complicated and time-consuming. Some of them may even have toxicity issues.¹⁶ As biocompatible alternatives, enzyme-assisted strategies have recently gained considerable interest for the sensitivity improvement of MB-based platforms.¹⁷ There are a great number of enzymes which can realize the signal amplification purpose, including nicking enzyme,¹⁸ polymerase,¹⁹ exonuclease III,²⁰ Cryonase,²¹ HaeIII nuclease,²² and duplex-specific nuclease.^{8,23} Nevertheless, some disadvantages may affect their wide applications. For instance, most enzymes are highly sequence-specific, which makes them only applicable to quite a limited number of cases. Furthermore, some enzymes can

^aDepartment of Chemistry, Zhejiang Sci-Tech University, Hangzhou 310008, P. R. China. E-mail: cui.liang@zjtu.edu.cn

^bBiomaterials Research Center, School of Biomedical Engineering, Southern Medical University, Guangzhou 510515, P. R. China. E-mail: jhuangaf@connect.ust.hk

† These authors contributed equally to this work.



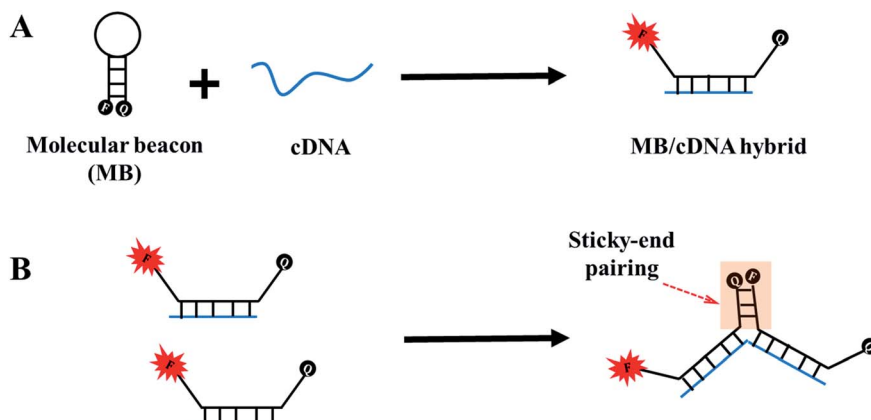


Fig. 1 The detection mechanism of a regular molecular beacon (MB) and the potential limitations during hybridization assays. (A) An MB molecule assumes a hairpin structure with a self-complementary stem whose ends are conjugated with a fluorophore (F) and quencher (Q) to allow fluorescence resonance energy transfer (FRET). In the presence of cDNA, cDNA binds to the MB's loop domain and forces the stem open that permits fluorescence recovery. This process shows how an MB works in the classic fluorescence detection system. It is noteworthy that the binding ratio between MBs and DNA targets is 1 : 1, which somehow, constrains the signal gain. (B) However, a problem encountered is that sticky-end pairing events may occur. If only the loop region is responsible for target recognition, MBs bound to cDNA make their two complementary ends change into sticky ends. The sticky ends between two different MB/cDNA hybrids tend to reassemble and then bring the fluorophore and quencher approaching each other again. This easily induces an unexpected signal drop in fluorescence and results in false-negative results. Proper measures should be taken to avoid the occurrence of sticky-end pairing phenomenon.

perform their functions in a universal means, but their corresponding hairpin DNA probes usually have to be deliberately designed, which makes it difficult to become popular. Therefore, it is highly demanded to construct new MB-based biosensors that are simple-to-implement and time-efficient, yet signal-amplifiable and sequence-specific.

Another issue is DNA sticky-end pairing among MBs that have already hybridized with target molecules,^{24,25} as depicted in Fig. 1B. This phenomenon usually takes place when MBs with long stem structures. When the loop portion of MBs bind with their targets, two arms of the stem structures convert into sticky ends. The sticky ends of MB/target complexes glue together, thus compelling the fluorescence donor and acceptor approaching each other and thereby permitting FRET again. Consequently, an unexpected fluorescence decrease is induced, leading to false-negative signals and poor detection quality. To avoid DNA sticky end pairing, one straightforward solution is to shorten the stem length of MBs. However, this makes the MBs unstable to form hairpin structures, thus generating high background signals. Another alternative measure is the employment of shared-stem MBs, which means that one arm of the stem region also participates in the hybridization to nucleic acid targets. The shared-stem design effectively prevents sticky end pairing events, accompanying by faster hybridization kinetics and higher signal gain.²⁶ Unfortunately, compared to conventional MBs, shared-stem MBs show reduced recognition specificity to discriminate mismatched targets.²⁷ Consequently, it remains a challenging task how to circumvent the influence from sticky-end pairing for reliable and accurate detection of target molecules.

With this regard, we herein describe a new fluorescence biosensor by using an intriguing MB, whose enzymatic behaviors can be transformed by the DNA target, as well as DNase I that can digest bound MBs for the amplification of response signal and the elimination of sticky-end pairing. In this work, 2'-O-methyl MBs and classic MBs are designed, prepared, and then their sensing

performances are compared. The interactions between MBs and DNase I before and after the addition of targets are intensively studied by using fluorescence analysis and polyacrylamide gel electrophoresis. An interesting finding is that the End-O-methyl MB can resist enzymatic digestion by DNase I that would otherwise occur upon the hybridization of End-O-methyl MB with a complementary DNA sequence. Based on this inspiring finding, we describe a new 2'-O-methyl MB-based and DNase I-assisted strategy for the amplified DNA detection, which is relatively convenient, rapid, and reliable. The detection platform consists of hairpin nucleic acid probes (End-O-methyl MBs) and nucleases (DNase I). There is no need for the separation and removal of unbound MBs. The assay is conducted in a mix-and-measure fashion and can be quickly completed. Upon the introduction of the target DNA, it hybridizes with the End-O-methyl MB, which, once bound, is transformed into accessible substrates for DNase I. The efficient digestion of End-O-methyl MBs by DNase I can subsequently generate a significant fluorescence enhancement related to the amounts of DNA targets. Therefore, this method is facile, fast, and robust, which may inspire the design and utilization of molecular probes in biomedical diagnosis.

Experimental section

Materials

DNase I and all relevant DNA sequences (see Table 1) were purchased from Takara Biotechnology Co. Ltd. (Dalian, China) and used without further purification. Stains All was purchased from Sigma-Aldrich (St. Louis, MO, USA).

Fluorescence measurement

Fluorescence measurements were carried out on a RF-5301-PC Fluorescence Spectrophotometer (Shimadzu, Japan).



Table 1 Sequences of oligonucleotides used in this study^{a,b}

Name	Sequence
Normal MB	5'-FAM-CATGA C AAC TAT ACA ACC TAC TA C CTC A G TCATG-Dabcyl-3'
End- <i>O</i> -methyl MB	5'-FAM-CATGA C AAC TAT ACA ACC TAC TA C CTC AG TCATG-Dabcyl-3'
All- <i>O</i> -methyl MB	5'-FAM-CATGA <i>C</i> AAC TAT ACA ACC TAC TA <i>C</i> CTC <i>A</i> G TCATG-Dabcyl-3'
cDNA	5'-TGA GGT AGT AGG TTG TAT AGT T-3'
smDNA	5'-TGA GGT AGT AG <u>A</u> TTG TAT AGT T-3'
tmDNA	5'-TGA GGT AGT <u>ATA</u> <u>CTG</u> TAT AGT T-3'
Random DNA	5'-GCA ACT TTG GCA TTC GGA ACT A-3'

^a Italic letters represent the 2'-*O*-methyl RNA bases. ^b Underlined letters indicate the mismatched sites.

Excitation and emission wavelengths were set at 490 and 520 nm, respectively, with 5 nm bandwidth. The emission spectra were measured by exciting samples at 490 nm and scanning the emission from 500 to 650 nm. All experiments were conducted in 20 mM Tris-HCl (pH 7.5) buffer with 5 mM MgCl₂ and 150 mM NaCl involved. The detection procedure was performed in 200 μL solution consisting of 100 nM MBs, 6.25 U mL⁻¹ DNase I, and various concentrations of DNA targets at room temperature for 30 min.

Gel electrophoresis

Eight tubes of 10 μM different MBs in 10 μL Tris-HCl buffer with and without the presence of cDNA after the addition of DNase I were prepared for 30 min at 37 °C. Afterwards, the samples were heated to 95 °C for 15 min to deactivate DNase I. A 20% denaturing polyacrylamide gel was prepared using 1× TBE buffer (pH 8.3). The gel was run at 1 W power for about one hour in 1× TBE buffer, stained for 30 min with Stains All solution (500 mL formamide, 100 mL 10× TBE, 400 mL H₂O, 200 mg Stains All), and finally pictures were taken by using a digital camera.

Results and discussion

Enhanced structural stability

There were three kinds of MBs designed and prepared (Table 1), including one normal MB with regular DNA bases, and another two *O*-methyl MBs with 2'-*O*-methyl RNA bases modified at only the stem parts (End-*O*-methyl MB) and the whole strand (All-*O*-methyl MB), respectively. The melting temperature (*T_m*), defined as the temperature at which half of the stem-loop probes are dissociated to random coil phase, is usually used to determine the thermal stability of DNA probes. To investigate the stem stability of MBs, the melting profiles of all MBs were recorded, as shown in Fig. 2. The *T_m* of each probe was characterized and compared. For all hairpin DNA probes, *O*-methyl MBs exhibited higher melting temperatures than the normal MB with the same sequences. For example, the End-*O*-methyl MB had a *T_m* of around 70.3 °C, which was much higher than that for the normal MB (49.1 °C). Maybe this is caused by the

incorporation of 2'-*O*-methyl oligoribonucleotides with a methoxy group at the 2' position of the sugar moiety instead of a hydrogen atom involved in natural oligodeoxribonucleotides.²⁸ For the All-*O*-methyl MB, its *T_m* (73.1 °C) was even higher than that of the End-*O*-methyl MB. This might be attributed to the substitution of more 2'-*O*-methyl RNA bases in the loop structures of All-*O*-methyl MBs.

The conditional resistance to enzyme digestion

To evaluate the enzymatic cleavage protection effect on MBs possessing 2'-*O*-methyl ribonucleotide backbones, DNase I was intentionally used to examine the enzymatic performances of all MBs. As depicted in Fig. 3A, normal MBs suffered severely from enzymatic cleavage, evidenced by the remarkable enhancement in fluorescence signal immediately after the introduction of DNase I. However, the End-*O*-methyl MBs displayed an amazing enzymatic resistance, since there was only a slight increase in the fluorescence signal. Interestingly, the All-*O*-methyl MB showed excellent resistance to nuclease digestion due to the fact that there was essentially no signal change after incubating with DNase I for more than 10 min. It is also noted that the background signal of normal MBs was much higher than those induced by *O*-methyl MBs. This was due to the higher binding affinity of *O*-methyl bases and better stem stability of *O*-methyl MBs,²⁸ which was also confirmed by the results in Fig. 2.

The addition of cDNA into all MBs could significantly affect the behaviors of MBs interacting with DNase I, as demonstrated in Fig. 3B. There was an insignificant fluorescence enhancement for normal MB/cDNA complex, indicating that further cleavage events were initiated by DNase I. But there was almost no signal difference for All-*O*-methyl MB/cDNA hybrids before and after the introduction of DNase I, which suggested extreme stability of All-*O*-methyl MBs. More importantly, the signal of the End-*O*-methyl MB hybridized with cDNA increased rapidly upon the addition of DNase I. This means that End-*O*-methyl

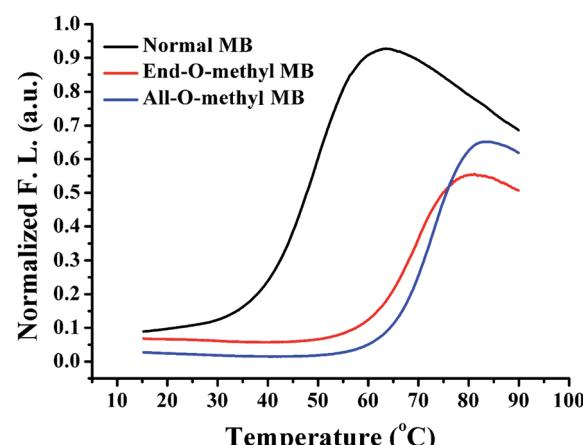


Fig. 2 Fluorescence melting profiles for all MBs, including normal MBs, End-*O*-methyl MBs, All-*O*-methyl MBs. The buffer solution contained 20 mM Tris-HCl (pH 7.5) with 150 mM NaCl and 5 mM MgCl₂. The temperature started from 15 °C and gradually increased to 95 °C.



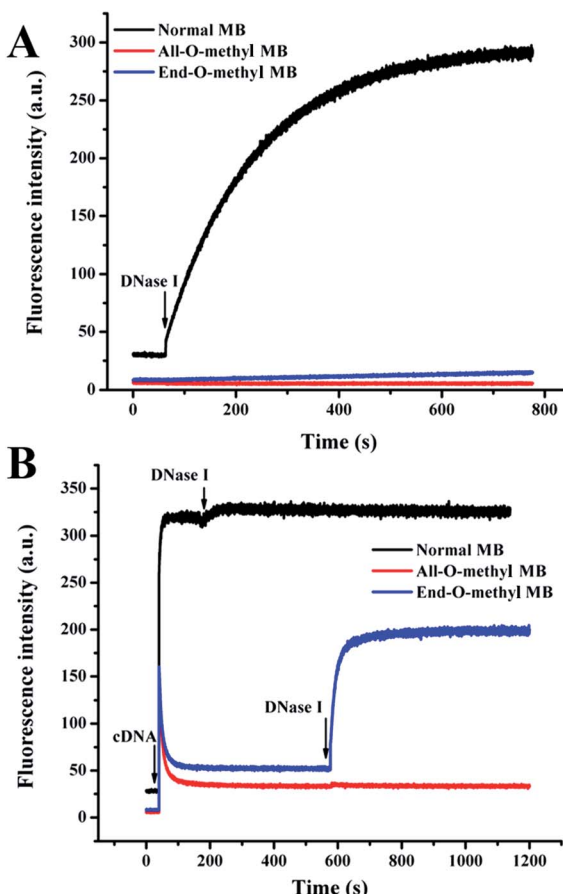


Fig. 3 Fluorescence responses of MBs interacting with DNase I before (A) and after (B) the addition of cDNA. The buffer solution contained 20 mM Tris-HCl (pH 7.5) with 150 mM NaCl and 5 mM MgCl₂.

MBs bound to DNA targets became vulnerable towards hydrolysis by DNase I that would otherwise were impervious to enzymatic digestion without the presence of DNA targets. The conditional digestion events of End-O-methyl MBs for DNase I might be caused by the preference of DNase I for double-stranded DNA, rather than single-stranded DNA. The activatable End-O-methyl MBs have profound impact on the design and application of enzyme-assisted amplified biosensing strategies.

It is noteworthy that for O-methyl MBs, there was an abnormal rapid decrease in fluorescence over time after the addition of cDNA (Fig. 3B). This signal drop indicated that sticky-end pairing events took place, as reported previously.²⁵ The reason might be that the 2'-O-methyl RNA bases possessed a higher affinity and faster hybridization kinetics than that of the natural DNA bases.^{26,28} Once opened, the two arms of O-methyl MBs had a high tendency of forming sticky-end pairing, thus bringing the fluorophore and quencher close to each other again, followed by a sudden drop in fluorescence during hybridization assays. This undesired signal decrease might give rise to false-negative results. Fortunately, the introduction of DNase I into the sensing system involving End-O-methyl MBs could result in a complete hydrolysis of MB/target duplexes,

which helped to release the fluorescence emission accurately related to the amounts of target molecules. The employment of DNase I was beneficial not only to the enhancement of response signal, but also to the removal of sticky-end pairing. The combination use of End-O-methyl MBs with DNase I made the amplified detection of DNA targets rational and feasible in this work.

The interaction mechanism of MBs with DNase I with and without the presence of cDNA was further confirmed by denatured polyacrylamide gel electrophoresis results (Fig. 4). The regular MBs could be efficiently digested by DNase I before (lane 3) and after (lane 4) the introduction of cDNA. In contrast, there was no detectable cleavage of All-O-methyl MBs after incubation with DNase I regardless of the presence of cDNA, as seen from lanes 7 and 8. It is noted that the initially inert End-O-methyl MBs (lane 5), once opened by cDNA, were transformed into effective substrates for DNase I (lane 6). Altogether, the results reveal that the All-O-methyl MBs would not be degraded by DNase I, while the End-O-methyl MBs bound to cDNA would be converted into accessible substrates for DNase I. This finding is of great significance for the development of enzyme-assisted, signal-enhanced biosensors. Therefore, the End-O-methyl MBs would be utilized to achieve accurate and reliable quantification of DNA targets with the assistance of DNase I in the following experiments.

Working mechanism

The detection principle is demonstrated in Scheme 1. The presence of cDNA forces MBs to be opened to achieve fluorescence recovery. However the newly exposed sticky ends of different MB/cDNA hybrids tend to re-organize and the fluorophore and quencher (Q) are brought into close proximity to cause fluorescence quenching again. This so-called sticky-end pairing usually gives rise to an undesired fluorescence decrease and thus generates false results. Fortunately, the addition of DNase I recognizes the MB/target complexes and triggers an effective cleavage, giving rise to the separation of fluorophore and quencher and thus producing a considerable signal enhancement, as depicted in Scheme 1. It should be

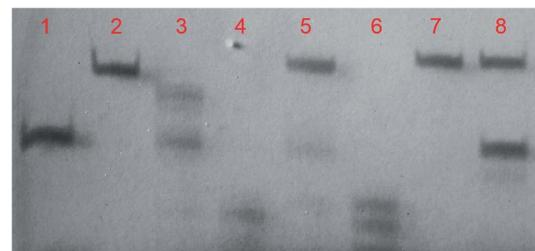
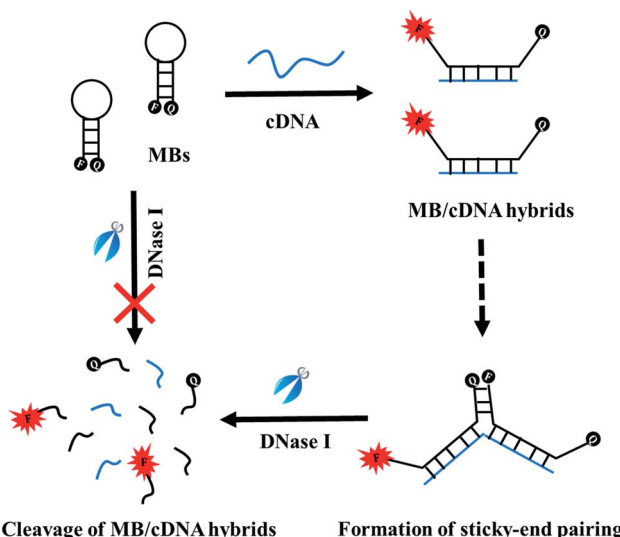


Fig. 4 Denatured polyacrylamide gel electrophoresis analysis of all MBs and cDNA with DNase I. Lane 1: cDNA; lane 2: normal MB; lane 3: normal MB with DNase I; lane 4: normal MB and cDNA with DNase I; lane 5: End-O-methyl MB with DNase I; lane 6: End-O-methyl MB and cDNA with DNase I; lane 7: All-O-methyl MB with DNase I; lane 8: All-O-methyl MB and cDNA with DNase I. The gel was run at 1 W power for 1 hour in 1× TBE buffer, stained for 30 min with Stains All solution (500 mL formamide, 100 mL 10× TBE, 400 mL H₂O, 200 mg Stains All).





Scheme 1 The scheme illustrating how End-O-methyl MBs and DNase I are used for the amplified detection of DNA targets, which can avoid the effects caused from sticky-end pairing. Upon the addition of cDNA, cDNA binds the MB. The MB/cDNA duplexes have a high tendency to trigger unexpected sticky-end pairing that may impede the accurate detection. Interestingly, the presence of DNase I can not only prevent the sticky-end pairing effects but also further liberate the fluorescence emission. This makes the reliable and accurate detection of DNA targets possible and rational.

mentioned that without the addition of target analytes, End-O-methyl MBs are inert to enzymatic digestion by DNase I.

The results in the aforementioned discussion parts support the hypothesis very well. In the absence of the target DNA, the End-O-methyl MB retained stable and its fluorescence signal remained unchanged even after the introduction of DNase I, as shown in Fig. 3A. However, when the target DNA appeared, it bound with the End-O-methyl MB, leading to the production of End-O-methyl MB/target complex. The products became the suitable substrates for DNase I, and then a complete digestion of MB was triggered and

a substantial fluorescence enhancement could be detected, as described in Fig. 3B. It should be mentioned that sticky-end did happen since an abnormal quick signal drop in fluorescence intensity was recorded, as shown in Fig. 3B.

In the detection scheme (Scheme 1), End-O-methyl MBs with switchable enzymatic performances are wisely used to ensure a greatly suppressed background signal yet hold promising potential for target recognition and a subsequent digestion by DNase I. The employment of DNase I is anticipated to dramatically magnify the fluorescence signal and efficiently circumvent the effects of sticky-end pairing, thereby ensuring sensitivity improvement.

Detection sensitivity

The detection limit was studied by varying the DNA target concentration from 75 pM to 50 nM, as seen in Fig. 5. Fig. 5A shows the fluorescence responses of the sensing platform upon the addition of DNA targets. It is found that the number of MBs opened by the target and subsequently cleaved by DNase I increased with elevated target concentration. The relationship of the fluorescence intensity with the target concentration is depicted in Fig. 5B. The limit of detection was calculated to be 27.4 pM according to the $3\sigma/\text{slope}$ rule. The detection limit of the conventional approach was about 5–10 nM, which is about 200-fold poorer than that of this new sensing strategy. These results together indicate that the remarkable sensitivity enhancement is indeed caused by the ingenious use of DNase I and the tailor-made End-O-methyl MBs. Meanwhile, this detection limit is also superior or comparable to the previous MB-based amplification methods (see Table 2).

Detection selectivity

The selectivity of was also tested by scrutinizing the sensing system with other DNA sequences containing mismatched bases, including single base-, three base-mismatched, and random DNA sequences (see Table 1). Fig. 6 shows the fluorescence differences 30 min after the addition of 10 nM DNA sequences. It is noticed that the fully matched DNA target

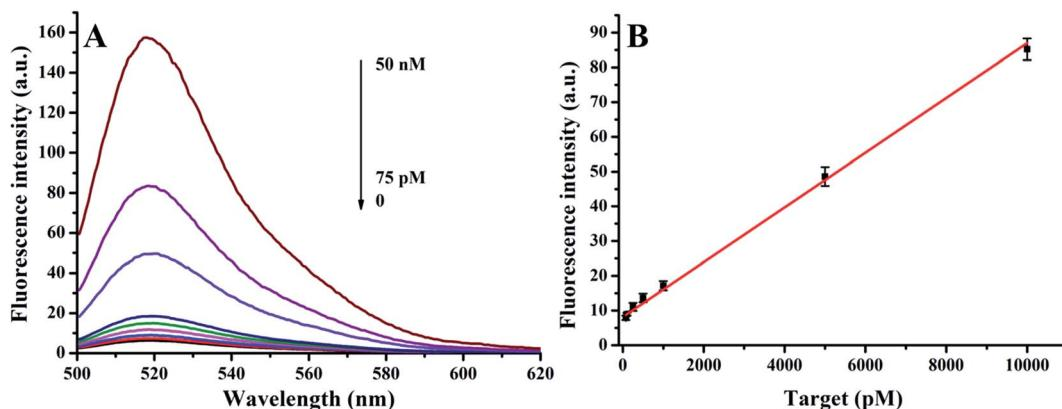


Fig. 5 Fluorescence response of 100 nM End-O-methyl MB with and without the presence of 6.25 U mL⁻¹ DNase I upon the addition of various concentrations of DNA targets. (A) Fluorescence emission spectra with the presence of DNase I. (B) The linear relationship between the fluorescence intensity at the emission wavelength of 520 nm as a function of target DNA concentration ranging from 0 to 10 nM. All the samples reacted at room temperature for 30 min before measurement. The buffer solution contained 20 mM Tris-HCl (pH 7.5) with 150 mM NaCl and 5 mM MgCl₂.



Table 2 Comparison of different nucleic acid sensing methods by using hairpin DNA probes and amplification mechanisms

Amplification element I (using nanomaterials)	Amplification element II (using enzymes)	Method	Detection limit	Ref.
Gold nanoparticles	—	Fluorescence	500 pM	29
Gold nanoparticles	—	Fluorescence	25 pM	30
Gold nanoparticles	—	Absorbance	200 pM	31
Gold nanoparticles	Duplex specific nuclease	Electrochemistry	0.17 pM	7
Carbon nanoparticles	DNase I	Fluorescence	3.2 pM	30
Graphene oxide	Exonuclease III	Fluorescence	1 pM	7
Graphene oxide	—	Fluorescence	2.0 nM	32
Graphene oxide	—	Fluorescence	75 pM	33
Carbon nanotubes	—	Fluorescence	4.0 nM	34
Carbon nanotubes	—	Fluorescence	42 pM	35
Carbon nanotubes/quantum dots	Nicking endonuclease	Fluorescence	30 fM	36
Molybdenum disulfide	—	Fluorescence	15 pM	9
Quantum dots	—	Fluorescence	0.76 pM	37
—	Exonuclease III	Fluorescence	10 pM	38
—	Nicking endonuclease	Fluorescence	50 fM	38
—	Nicking endonuclease	Fluorescence	6.2 pM	39
—	Duplex specific nuclease	Fluorescence	1.03 pM	40
—	DNase I	Fluorescence	27.4 pM	This work

produced a considerably stronger fluorescence signal compared with those triggered by mismatched DNA sequences. The satisfactory detection specificity was attributed to the relatively higher energy barrier set by the more stable stems of End-*O*-methyl MBs, as well as the accurate recognition capability of DNase I towards End-*O*-methyl MB/cDNA complex.

It is noted that compared with natural oligoribonucleotide probes, 2'-*O*-methyl nucleic acid probes exhibit superior properties, including faster hybridization kinetics, better signal-to-background ratios, remarkably elevated T_m values, and improved binding specificity.^{28,41} Therefore, 2'-*O*-methyl nucleic acid probes have emerged as powerful molecular tools for the assays of nucleic acids, such as the detection of RNA,⁴² the visualization of RNA in living cells,⁴³ and imaging dynamic mRNA processes in living cells,⁴⁴ and so on. Other than 2'-*O*-

methyl nucleic acid probes, there are also some other kinds of promising nucleic acid probes, such as locked nucleic acids (LNA),⁴⁵ peptide nucleic acids (PNA),⁴⁶ and (L)-DNA.⁴⁷

Conclusions

In summary, an innovative End-*O*-methyl MB-mediated sensing method was proposed for amplified fluorescence detection of DNA targets in a simple, sensitive, and selective manner. It took advantage of the fascinating properties of End-*O*-methyl MBs, including enhanced thermal stability (that was able to substantially reduce background signal) and exceptional nuclease resistance (that could guarantee the detection performance by eliminating the undesired cleavage of MBs). A noteworthy finding is that the coupling use of *O*-methyl MBs and DNase I could eliminate the sticky-end pairing effect and amplify the response signal. A detection sensitivity could be easily obtained as 27.4 pM, which was nearly two orders of magnitude better than the conventional MB-based strategy. It also showed good selectivity. Overall, the merits aforementioned make the proposed method potentially beneficial for the advances in the fields of life science, analytical chemistry, biomedical engineering, and clinical diagnosis.

Conflicts of interest

The authors declare no conflict of interest.

Acknowledgements

This work was financially supported by Zhejiang Provincial Natural Science Foundation of China (No. LY19B050009) and the National Natural Science Foundation of China (No. 21705076 and 21975117).

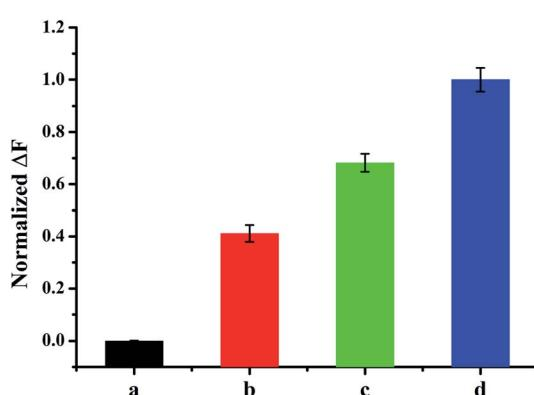


Fig. 6 Detection selectivity investigation of the proposed sensing method against mismatched DNA sequences. The concentration of all matched and mismatched DNA targets was 10 nM. Samples a, b, c, and d were random DNA, tmDNA, smDNA, and cDNA, respectively. All the samples reacted at room temperature for 30 min before measurement. The buffer solution contained 20 mM Tris–HCl (pH 7.5) with 150 mM NaCl and 5 mM MgCl₂.



References

1 D. M. Kolpashchikov, *Chem. Rev.*, 2010, **110**, 4709–4723.

2 Q. Li, G. Luan, Q. Guo and J. Liang, *Nucleic Acids Res.*, 2002, **30**, E5.

3 W. F. Lv, J. M. Zhao, B. Situ, B. Li, W. Ma, J. M. Liu, Z. X. Wu, W. Wang, X. H. Yan and L. Zheng, *Biosens. Bioelectron.*, 2016, **83**, 250–255.

4 K. M. Wang, Z. W. Tang, C. Y. J. Yang, Y. M. Kim, X. H. Fang, W. Li, Y. R. Wu, C. D. Medley, Z. H. Cao, J. Li, P. Colon, H. Lin and W. H. Tan, *Angew. Chem., Int. Ed.*, 2009, **48**, 856–870.

5 J. H. Huang, X. F. Su and Z. G. Li, *Sens. Actuators, B*, 2014, **200**, 117–122.

6 J. H. Huang, Z. Y. Wang, J. K. Kim, X. F. Su and Z. G. Li, *Anal. Chem.*, 2015, **87**, 12254–12261.

7 Y. Y. Tao, D. Yin, M. C. Jin, J. Fang, T. Dai, Y. Li, Y. X. Li, Q. L. Pu and G. M. Xie, *Biosens. Bioelectron.*, 2017, **96**, 99–105.

8 Q. Zhao, J. F. Piao, W. P. Peng, Y. Wang, B. Zhang, X. Q. Gong and J. Chang, *ACS Appl. Mater. Interfaces*, 2018, **10**, 3324–3332.

9 J. H. Huang, L. Ye, X. Gao, H. Li, J. B. Xu and Z. G. Li, *J. Mater. Chem. B*, 2015, **3**, 2395–2401.

10 M. S. Xiao, T. T. Man, C. F. Zhu, H. Pei, J. Y. Shi, L. Li, X. M. Qu, X. Z. Shen and J. Li, *ACS Appl. Mater. Interfaces*, 2018, **10**, 7852–7858.

11 X. P. Wei, S. Su, Y. Y. Guo, X. X. Jiang, Y. L. Zhong, Y. Y. Su, C. H. Fan, S. T. Lee and Y. He, *Small*, 2013, **9**, 2493–2499.

12 X. Su, C. Zhang and M. P. Zhao, *Biosens. Bioelectron.*, 2011, **26**, 3596–3601.

13 Q. M. Feng, Y. Z. Shen, M. X. Li, Z. L. Zhang, W. Zhao, J. J. Xu and H. Y. Chen, *Anal. Chem.*, 2016, **88**, 937–944.

14 Z. P. Zhou, H. D. Huang, Y. Chen, F. Liu, C. Z. Huang and N. Li, *Biosens. Bioelectron.*, 2014, **52**, 367–373.

15 J. H. Huang, Q. B. Zheng, J. K. Kim and Z. G. Li, *Biosens. Bioelectron.*, 2013, **43**, 379–383.

16 E. Bergamaschi, C. Poland, I. G. Canu and A. Prina-Mello, *Nano Today*, 2015, **10**, 274–277.

17 I. Iwe, Z. G. Li and J. H. Huang, *Microchim. Acta*, 2019, **186**, 716.

18 W. T. Xu, C. G. Wang, P. Y. Zhu, T. X. Guo, Y. C. Xu, K. L. Huang and Y. B. Luo, *Analyst*, 2016, **141**, 2542–2552.

19 A. R. Connolly and M. Trau, *Angew. Chem., Int. Ed.*, 2010, **49**, 2720–2723.

20 C. J. Yang, L. Cui, J. H. Huang, L. Yan, X. Y. Lin, C. M. Wang, W. Y. Zhang and H. Z. Kang, *Biosens. Bioelectron.*, 2011, **27**, 119–124.

21 Y. F. Lou, Y. B. Peng, X. Luo, Z. Yang, R. Wang, D. Sun, L. Li, Y. Tan, J. Huang and L. Cui, *Microchim. Acta*, 2019, **186**, 494.

22 X. L. Feng, L. B. Liu, Q. Yang and S. Wang, *Chem. Commun.*, 2011, **47**, 5783–5785.

23 K. Zhang, K. Wang, X. Zhu, M. H. Xie and X. L. Zhang, *Biosens. Bioelectron.*, 2017, **87**, 299–304.

24 E. Winfree, F. Liu, L. A. Wenzler and N. C. Seeman, *Nature*, 1998, **394**, 539–544.

25 J. J. Li and W. Tan, *Anal. Biochem.*, 2003, **312**, 251–254.

26 C. J. Yang, L. Wang, Y. Wu, Y. Kim, C. D. Medley, H. Lin and W. Tan, *Nucleic Acids Res.*, 2007, **35**, 4030–4041.

27 A. Tsourkas, M. A. Behlke and G. Bao, *Nucleic Acids Res.*, 2002, **30**, 4208–4215.

28 A. Tsourkas, M. A. Behlke and G. Bao, *Nucleic Acids Res.*, 2002, **30**, 5168–5174.

29 S. P. Song, Z. Q. Liang, J. Zhang, L. H. Wang, G. X. Li and C. H. Fan, *Angew. Chem., Int. Ed.*, 2009, **48**, 8670–8674.

30 Y. J. Yang, J. Huang, X. H. Yang, X. X. He, K. Quan, N. L. Xie, M. Ou and K. M. Wang, *Anal. Chem.*, 2017, **89**, 5851–5857.

31 K. Quan, J. Huang, X. H. Yang, Y. J. Yang, L. Ying, H. Wang and K. M. Wang, *Analyst*, 2015, **140**, 1004–1007.

32 C. H. Lu, J. Li, J. J. Liu, H. H. Yang, X. Chen and G. N. Chen, *Chemistry*, 2010, **16**, 4889–4894.

33 J. Huang, X. H. Yang, X. X. He, K. M. Wang, Y. He and K. Quan, *Chem. Commun.*, 2013, **49**, 9827–9829.

34 R. H. Yang, J. Y. Jin, Y. Chen, N. Shao, H. Z. Kang, Z. Xiao, Z. W. Tang, Y. R. Wu, Z. Zhu and W. H. Tan, *J. Am. Chem. Soc.*, 2008, **130**, 8351–8358.

35 J. Chen, Y. Huang, M. Shi, S. L. Zhao and Y. C. Zhao, *Talanta*, 2013, **109**, 160–166.

36 G. L. Wang, X. Fang, X. M. Wu, X. L. Hu and Z. J. Li, *Biosens. Bioelectron.*, 2016, **81**, 214–220.

37 X. L. Deng, C. Wang, Y. Gao, J. W. Li, W. Wen, X. H. Zhang and S. F. Wang, *Biosens. Bioelectron.*, 2018, **105**, 211–217.

38 X. L. Zuo, F. Xia, Y. Xiao and K. W. Plaxco, *J. Am. Chem. Soc.*, 2010, **132**, 1816–1818.

39 J. W. J. Li, Y. Z. Chu, B. Y. H. Lee and X. L. S. Xie, *Nucleic Acids Res.*, 2008, **36**, e36.

40 Y. C. Li, J. Y. Zhang, J. J. Zhao, L. K. Zhao, Y. Q. Cheng and Z. P. Li, *Analyst*, 2016, **141**, 1071–1076.

41 M. MAjlessi, N. C. Nelson and M. M. Becker, *Nucleic Acids Res.*, 1998, **26**, 2224–2229.

42 O. A. Krashenina, D. S. Novopashina, A. A. Lomzov and A. G. Venyaminova, *ChemBioChem*, 2014, **15**, 1939–1946.

43 C. Molenaar, S. A. Marras, J. C. M. Slats, J.-C. Truffert, M. Lemaitre, A. K. Raap, R. W. Dirks and H. J. Tanke, *Nucleic Acids Res.*, 2001, **29**, e89.

44 I. E. Catrina, S. A. E. Marras and D. P. Bratu, *ACS Chem. Biol.*, 2012, **7**, 1586–1595.

45 P. Bakthavatsalam, G. Longatte, S. O. Jensen, M. Manefield and J. J. Gooding, *Sens. Actuators, B*, 2018, **268**, 255–263.

46 J. C. Wu, Y. Zou, C. Y. Li, W. Sicking, I. Plantanida, T. Yi and C. Schmuck, *J. Am. Chem. Soc.*, 2012, **134**, 1958–1961.

47 G. L. Ke, C. M. Wang, Y. Ge, N. F. Zheng, Z. Zhu and C. J. Yang, *J. Am. Chem. Soc.*, 2012, **134**, 18908–18911.

